

## Binding Studies on CB[6] with a Series of 1-Alkyl-3-methylimidazolium Ionic Liquids in an Aqueous System

Nan Zhao, Li Liu, Frank Biedermann, and Oren A. Scherman\*<sup>[a]</sup>

*Dedicated to the 150th anniversary of Japan–UK diplomatic relations*

**Abstract:** The host–guest chemistry between a series of 1-alkyl-3-methylimidazolium bromide ( $[C_n\text{mim}]\text{Br}$ ) guests and the macrocyclic host molecule cucurbit[6]uril (CB[6]) in an aqueous system is systematically studied in neutral aqueous media. Both 1D and 2D NMR experiments in conjunction with isothermal titration calorimetry (ITC) unveil the binding characteristics of the host–guest interaction. Solution binding constants ( $K_a$ ) up to  $10^5\text{M}^{-1}$  are measured directly. Additionally, this

$[C_n\text{mim}]\text{Br}$ –CB[6] interaction was found to significantly increase the solubility of CB[6] in neutral water, in some cases by at least four orders of magnitude. From these studies, a detailed host–guest binding model has been constructed and is fully discussed.

**Keywords:** host–guest systems • macrocycles • NMR spectroscopy • ionic liquids • supramolecular chemistry

In this model, the delocalized positive charge on the imidazolium ring becomes partially localized on either one of the nitrogen atoms upon complexation with CB[6]. Localization of the positive charge is directly related to the length of the “1-alkyl” chain on the imidazolium ring, which causes an induced local dipole subsequently allowing for an ion–dipole interaction with the carbonyl portal of CB[6].

### Introduction

Cucurbit[6]uril (CB[6]) is a unique macrocyclic host molecule consisting of six glycoluril units and twelve methylene bridges (Figure 1).<sup>[1,2]</sup> Its rigid hydrophobic cavity and two hydrophilic portals make CB[6] an interesting and promising

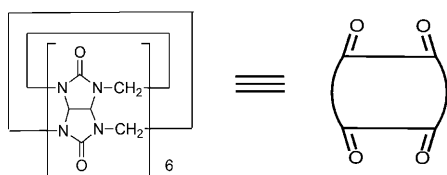


Figure 1. The molecular structure of CB[6].

supramolecular building block.<sup>[3–7]</sup> While some of the larger CB[ $n$ ] macrocyclic hosts<sup>[8]</sup> such as CB[7], CB[8], CB[10], and CB[ $n$ ] derivatives<sup>[9]</sup> have received increasing interest, CB[6] is still studied on account of its economical and facile synthesis and purification.

Although CB[6] has very poor solubility in water ( $\leq 0.018\text{mM}$ ),<sup>[10]</sup> host–guest binding studies in acidic solution ( $\text{HCO}_2\text{H}/\text{H}_2\text{O}$  (1:1 v/v)) have been successfully conducted since the 1980s.

Buschmann et al. reported weak binding between CB[6] and aliphatic alcohols, acids, and nitriles in  $\text{HCO}_2\text{H}/\text{H}_2\text{O}$  (1:1).<sup>[11]</sup> Binding constants as low as  $10^2$ – $10^3\text{M}^{-1}$  were reported and no sign of guest selectivity was observed. On the other hand, Mock and co-workers reported that charged ammonium molecules are good guests for CB[6].<sup>[12]</sup> The positive charge of ammonium interacts through ion–dipole interactions with the CB[6] portal carbonyl groups, thereby stabilizing the host–guest complexes. For mono-alkyl ammonium cations, the binding affinity varied from  $10^2$  to  $10^5\text{M}^{-1}$ , indicative of guest selectivity for different chain lengths.<sup>[13]</sup>

Kim et al. reported that CB[6] could also be dissolved in aqueous saline solutions.<sup>[14]</sup> X-ray crystallography indicated that multiple sodium ions interacted with the CB[6] portal carbonyls acting as a “lid” on the CB[6] barrel to control

[a] N. Zhao, Dr. L. Liu, F. Biedermann, Dr. O. A. Scherman  
Melville Laboratory for Polymer Synthesis  
Department of Chemistry  
University of Cambridge  
Cambridge, CB2 1EW (UK)  
Fax: (+44) 1223-334866  
E-mail: oas23@cam.ac.uk

Supporting information for this article is available on the WWW under <http://dx.doi.org/10.1002/asia.200900510>.

the binding and release of THF molecules from within the hydrophobic cavity. Buschmann measured the binding constants of CB[6] with a variety of alkali-metal, alkaline-earth, transition-metal, and lanthanide cations. Their binding constants are in the range of  $10^2$ – $10^3 \text{ M}^{-1}$  in acidic solution.<sup>[15–21]</sup> It is important to note that in acidic solution, protons are in constant competition with the metal cations, therefore, the actual binding constants between CB[6] and metal cations are likely to be higher than the measured values reported.<sup>[21,22]</sup>

Recently, we reported that 1*N*,3*N*-dialkylimidazolium, can act as a new guest and simultaneously serve to dissolve CB[6] in neutral water without the assistance of metal cations.<sup>[23]</sup> 1*N*,3*N*-dialkylimidazolium is a room-temperature ionic liquid (RTIL) which has attracted attention as a new solvent on account of its outstanding physical-chemical properties.<sup>[24,25]</sup> The properties of imidazolium RTILs can be readily tuned by simply mixing with different organic solvents or water. Many chemical reactions have been carried out in imidazolium–water mixtures. One example in particular was reported by Rault-Berthelot et al. where hydrogen could be generated in situ from the imidazolium–water mixture.<sup>[26]</sup>

Within the realm of CB chemistry, imidazolium RTILs are promising guests as their physical properties can be altered in a straightforward manner by varying both counter ion and the chemical nature of the alkyl substituents. These alterations yield a large variety of guests which are both simple to design and prepare.<sup>[27]</sup> A major difference between imidazolium cations and alkyl ammonium cations is that the positive charge on the former can be delocalized over 2.5 Å between the two nitrogen atoms in the five membered ring as illustrated in Figure 2.<sup>[28]</sup>

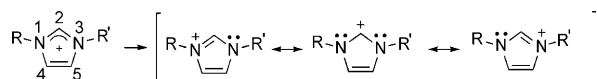


Figure 2. Resonance of an imidazolium cation.<sup>[28]</sup>

Several other groups have become interested in CB–imidazolium host–guest systems as well. Istvan et al. investigated the binding properties of imidazolium with CB[7].<sup>[29]</sup> Macartney et al. reported a decrease in H/D exchange rate for the acidic C2 proton on the imidazolium ring upon complexing with CB[7].<sup>[30]</sup> Schmitzer et al. found that 1*N*,3*N*-disubstituted methylenediimidazolium salts complex with CB[7] as well as several other host molecules.<sup>[31]</sup> Some of those diimidazolium guests were observed to form ternary complexes with CB[7] and cyclodextrins (CDs),<sup>[32]</sup> and some polyimidazolium cations containing aromatic binding sites could form [2]- and [3]-pseudorotaxanes

with CB[7].<sup>[33]</sup> Sindelar et al. reported two crystal structures for ethyl and butyl methylimidazolium with CB[6] which verify our proposed flexible binding model.<sup>[34]</sup> Very recently, we reported that 1*N*,3*N*-dimethylimidazolium methylsulphonate could be utilized to isolate a lid-free and charge-free CB[6]–diethyl ether inclusion complex.<sup>[35]</sup> However, a systematic study of CB[6] binding with different *N*1-alkyl chain lengths has not been probed until now. Herein, we investigate how varying the *N*1 alkyl chains from ethyl to octyl as well as dodecyl, affect CB[6] complexation. We also propose a complete binding model which can serve as a guideline for future work in this area.

## Results and Discussion

A series of imidazolium salts ranging from 1-ethyl-3-methylimidazolium bromide ([C<sub>2</sub>mim]Br) to 1-octyl-3-methylimidazolium bromide ([C<sub>8</sub>mim]Br) and 1-dodecyl-3-methylimidazolium bromide ([C<sub>12</sub>mim]Br) were synthesized and complexed with CB[6] in aqueous solution. While the counter ion can certainly have a dramatic effect on solubility and complexation, these effects are beyond the scope of this study and will be reported elsewhere. In order to eliminate any effects from counter-ion binding, all imidazolium guest molecules in this study contain a bromide counter ion. 1D, 2D NMR spectroscopy, and ITC characterization techniques were used to study the binding dynamics.

In NMR studies of the CB[6]–imidazolium systems, at least three factors influence the guest's chemical shifts: charge localization on the imidazolium ring, guest location inside the CB[6] cavity, and the rates of complexation and decomplexation. These factors are interdependent in determining the final guest chemical shift values. As the effects of complexation and decomplexation rates are well understood, only the first two effects are discussed below.

The positive charge on an imidazolium ring has an inductive effect on nearby atoms. When the charge partially localizes at the *N*3 atom (Figure 3 a), the chemical shifts of H<sub>a</sub> and H<sub>c</sub> will move downfield owing to greater withdrawing of electron density. In addition, H<sub>d</sub> and H<sub>e</sub> will shift upfield. When the positive charge is partially located at the *N*1 atom (Figure 3 b), the contrary is observed. For H<sub>b</sub>, no charge effect is observed. Thus, the chemical shift variation of H<sub>b</sub> arises from its relative location within CB[6], providing an insight into the binding geometry of the host–guest complex.

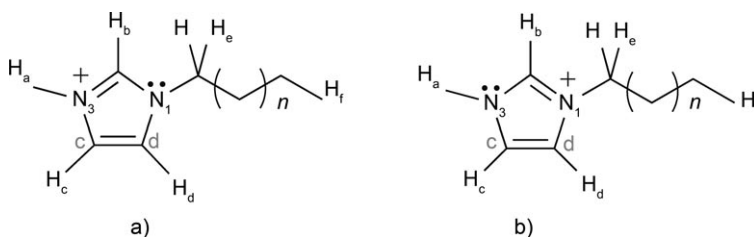


Figure 3. a) Positive charge partially located on *N*3, and b) positive charge partially located on *N*1.

The cavity of CB[6] provides high electron density which shields protons inside. The urea groups at the portal regions also cause magnetic shielding to the proximal guest protons by the presence of  $\pi$  electrons. Taking into account these effects, the shielding (deep grey) and deshielding (light grey) regions of CB[6] are shown in Figure 4.

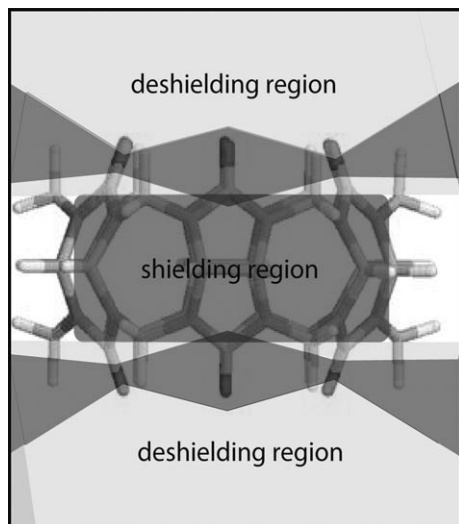


Figure 4. Shielding and deshielding regions of CB[6].

### 1D and 2D NMR Studies

Figure 5 is a stack plot of  $^1\text{H}$  NMR spectra of CB[6] with [C<sub>2</sub>mim]Br in neutral water. This host-guest system is in fast exchange. When binding with CB[6], H<sub>e</sub> and H<sub>f</sub> of

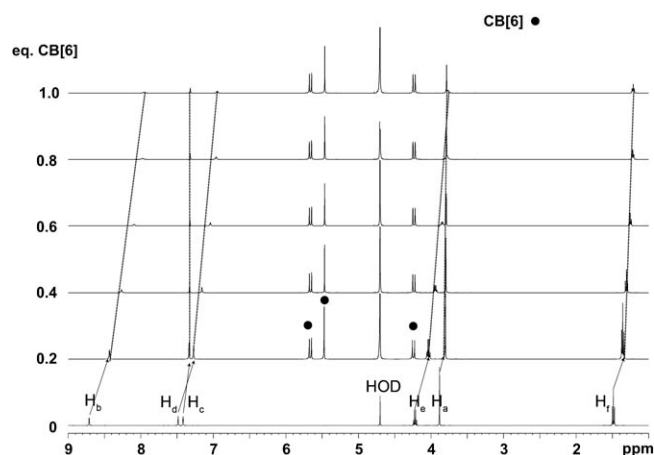


Figure 5.  $^1\text{H}$  NMR stack plot of CB[6] and [C<sub>2</sub>mim]Br in D<sub>2</sub>O with the “intended” ratios of 0, 0.2, 0.4, 0.6, 0.8, and 1.0 equivalent of CB[6].

[C<sub>2</sub>mim]Br move upfield which indicate that the ethyl chain on N1 goes inside the CB[6] cavity. The upfield shift of H<sub>b</sub> suggests that at least half of the five member ring is embedded inside CB[6]’s shielding region. Unfortunately, the H<sub>c</sub>/H<sub>d</sub> peaks are difficult to distinguish from 1D NMR alone.

Therefore, several 2D NMR techniques were employed to confirm our proton assignments.

Figure 6a and b are different regions of HMBC spectrum of [C<sub>2</sub>mim]Br in water. H<sub>a</sub> (singlet) and H<sub>e</sub> (quartet) are easily assigned as shown. H<sub>a</sub> has a larger correlation with C<sub>e</sub>

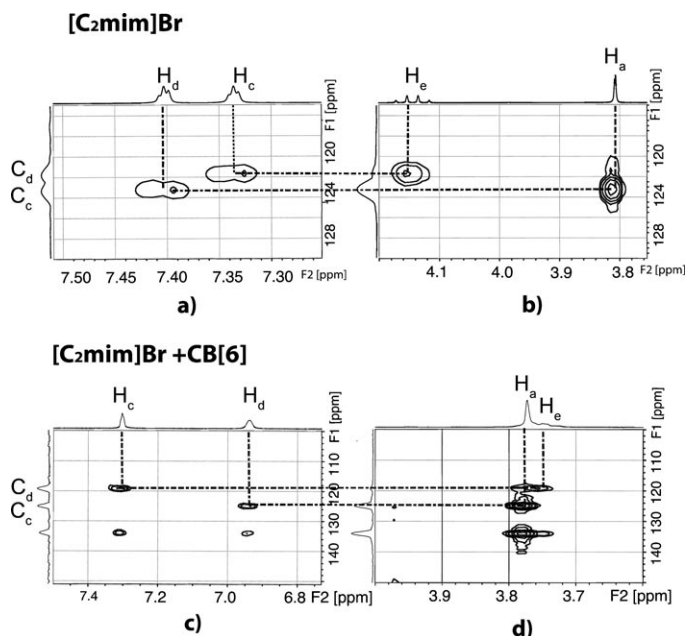


Figure 6. (a) and (b) HMBC spectra of [C<sub>2</sub>mim] Br. (c) and (d) HMBC spectra of [C<sub>2</sub>mim]Br in the presence of CB[6].

than C<sub>d</sub> ( $J^{3,CH} > J^{4,CH}$ ) while H<sub>e</sub> has a larger correlation with C<sub>d</sub> (Figure 6b). As a result, C<sub>c</sub> and C<sub>d</sub> are assigned and C<sub>c</sub> (124 ppm) is shifted about 2 ppm downfield from C<sub>d</sub> (122 ppm). In Figure 6a, C<sub>c</sub> correlates with H<sub>d</sub> and C<sub>d</sub> correlates with H<sub>c</sub>, allowing for the unambiguous assignment of H<sub>d</sub> and H<sub>c</sub> in the  $^1\text{H}$  NMR spectra in Figure 5. When CB[6] was added into the system (guest to host ratio is 3:1 according to integration), the same method was used to assign H<sub>c</sub> and H<sub>d</sub>. Different regions of the HMBC spectrum are shown in Figure 6c and d. Results show that H<sub>d</sub> (6.98 ppm) now moves upfield of H<sub>c</sub> (7.30 ppm).

NOESY was also employed to independently verify the correct assignment of H<sub>c</sub> and H<sub>d</sub>. Figure 7a is a region of the NOESY spectrum of [C<sub>2</sub>mim]Br in water. Compared to H<sub>d</sub>, H<sub>c</sub> is much closer to H<sub>a</sub> while H<sub>e</sub> is closer to H<sub>d</sub>. Therefore, once H<sub>a</sub> and H<sub>e</sub> have been determined, H<sub>d</sub> and H<sub>c</sub> are easily assigned. Figure 7b shows the NOESY signals of [C<sub>2</sub>mim]Br binding with CB[6]. The same method was employed to assign H<sub>c</sub> and H<sub>d</sub> and the result is consistent with that of the HMBC method discussed above.

Figure 8 is a stack plot of  $^1\text{H}$  NMR spectra of CB[6] with [C<sub>3</sub>mim]Br in water. This host-guest system exhibits fast exchange and the N1 alkyl chain was buried inside CB[6]’s cavity as indicated by protons H<sub>e</sub> and H<sub>f</sub>. However, in contrast to the CB[6]–[C<sub>2</sub>mim]Br system, H<sub>b</sub> and H<sub>d</sub> on the imidazolium ring move downfield while H<sub>c</sub> moves upfield. For

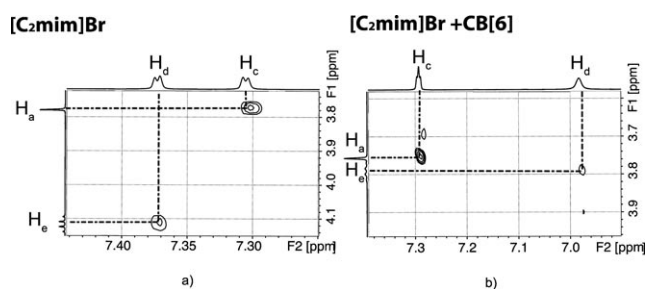


Figure 7. NOESY spectra of a)  $[C_2mim]Br$  and b)  $[C_2mim]Br$  binding with  $CB[6]$ .

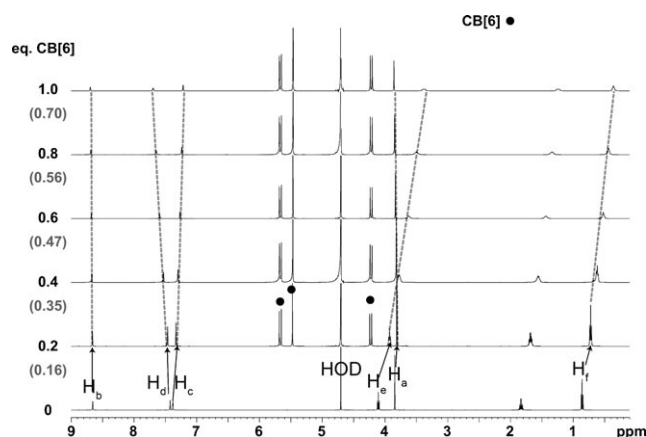


Figure 8.  $^1H$  NMR stack plots of  $CB[6]$  and  $[C_3mim]Br$  in  $D_2O$  with the "intended" ratios of 0, 0.2, 0.4, 0.6, 0.8 and 1.0 equivalent of  $CB[6]$ . Values in brackets are the real ratios from integration under intended ratio.

the remainder of the  $[C_nmim]Br$  series binding with  $CB[6]$  (for  $^1H$  NMR titration plots and typical HMBC and NOESY spectra of these  $CB[6]$ -imidazolium bindings, see Supporting Information), the imidazolium protons shift in an analogous manner to those for  $[C_3mim]Br$  except in the case of  $[C_{12}mim]Br$ .

Figure 9 shows the stack plot of  $^1H$  NMR spectra of  $CB[6]$  with  $[C_{12}mim]Br$  in water. Besides the fast exchange mode, it is noticeable that proton  $H_b$  shifts upfield as in the case of  $[C_2mim]Br$ . Some of the protons on the N1 alkyl chain shift downfield while other protons shift upfield, clearly indicating that the alkyl chain is not fully buried inside  $CB[6]$ 's cavity. A conformational rearrangement of the alkyl chain is likely to occur, similar to what has been observed previously by Kim and co-workers for the larger  $CB[8]$  homologue.<sup>[36]</sup> A more detailed investigation of these dynamics is currently underway.

Under a 1:1 *intended* guest/host ratio, the chemical shift variation of the bound guest

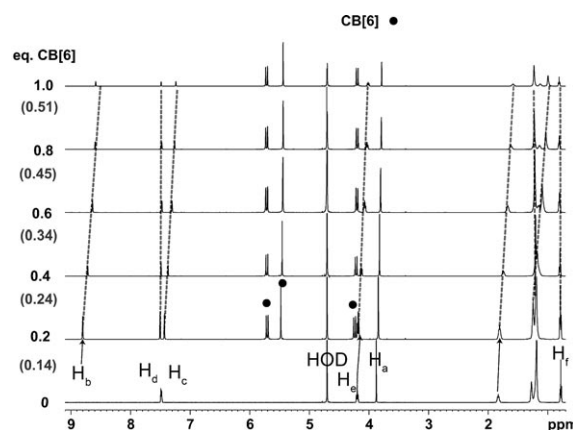


Figure 9.  $^1H$  NMR stack plots of  $CB[6]$  and  $[C_{12}mim]Br$  in  $D_2O$  with the "intended" ratios of 0, 0.2, 0.4, 0.6, 0.8 and 1.0 equivalent of  $CB[6]$ . Values in brackets are the real ratios from integration under intended ratio.

from free guest was recorded and listed in Table 1. These numbers indicated the shielding or deshielding effects on the guest protons upon binding with  $CB[6]$ . Negative values indicate shielding upon binding, while positive values indicate deshielding. In Table 1,  $[H]_r/[G]_r$  shows the *real* ratio in solution based on integration of the  $^1H$  NMR spectrum while the *intended* ratio was 1:1. These ratios indicate the guests' ability to solubilize  $CB[6]$  into water. With the same guest concentration,  $[C_4mim]Br$  and  $[C_3mim]Br$  can bring an equimolar amount of  $CB[6]$  into solution, showing strong binding affinities between host and guest. When the N1 chain lengths increase or decrease, the host concentration in solution decreases and the binding mode is always fast exchange, which correlates with a weaker host-guest interaction.

In each case, protons on the N1 alkyl chain move upfield indicating cavity binding. It is important to mention that for  $[C_7mim]Br$  and  $[C_8mim]Br$ , the upfield shifts of  $H_f$  (the terminal  $CH_3$  protons) indicate that the whole heptyl or octyl chain is inside  $CB[6]$ . As the heptyl and octyl chains are longer than the depth of the  $CB[6]$  cavity, a conformational rearrangement of the alkyl chain inside the  $CB[6]$  cavity must take place. For the chain end of  $[C_{12}mim]Br$ , a slight downfield variation was observed for  $H_f$  indicating the chain end likely lies outside the cavity of  $CB[6]$ .

Table 1. Complexation induced chemical shift data in ppm for  $[C_nmim]Br-CB[6]$  in  $D_2O$  at  $25^\circ C$ .

$[C_nmim]Br$	$H_a$	$H_b$	$H_c$	$H_d$	$H_e$	$H_f$	$[H]_r/[G]_r$	exchange mode
$[C_2mim]Br$	-0.10	-0.76	-0.10	-0.54	-0.46	-0.27	0.46	fast
$[C_3mim]Br$	0.02	0.04	-0.16	0.27	-0.73	-0.50	0.70	fast
$[C_4mim]Br$	0.07	0.40	-0.16	0.58	-0.84	-0.70	1	slow
$[C_5mim]Br$	0.05	0.32	-0.14	0.35	-0.39	-0.60	1	slow
$[C_6mim]Br$	— <sup>[a]</sup>	0.14	-0.06	0.14	-0.02	-0.48	0.91	intermediate
$[C_7mim]Br$	0.02	0.11	-0.05	0.10	-0.01	-0.21	0.74	fast
$[C_8mim]Br$	-0.02	0.11	-0.10	0.09	-0.05	-0.13	0.65	fast
$[C_{12}mim]Br$	-0.05	— <sup>[a]</sup>	— <sup>[a]</sup>	0.10	-0.01	0.12	0.51	fast

[a] Value could not be measured.

## Host–Guest Binding Constants and Stoichiometry Studies

In host–guest chemistry, both binding stoichiometry and association constants are crucial to the understanding of host–guest binding events. The most common methods to determine these are titration experiments using spectroscopic methods such as  $^1\text{H NMR}$ , UV/Vis and fluorescence.<sup>[38]</sup> As the CB[6]-imidazolium UV/Vis absorption mechanism is not yet understood,  $^1\text{H NMR}$  titration methods were employed as a first attempt to understand the binding. Unfortunately, repeated titrations in an attempt to construct a Job plot proved impossible. This was likely to arise from the insolubility of CB[6] in the absence of the imidazolium guest, preventing us from obtaining any starting points. Fortunately, ITC was found to be a useful and relatively convenient method to obtain both the binding stoichiometry and association constants.

In a typical ITC experiment, CB[6] and  $[\text{C}_n\text{mim}]\text{Br}$  were dissolved in separate 10 mM phosphate buffer solutions (pH 7) and the binding experiments were carried out at 25 °C. Binding stoichiometry and thermodynamic data were obtained and are listed in Table 2 depicting a clear trend of

Table 2. Binding constants and thermodynamic data for  $[\text{C}_n\text{mim}]\text{Br}$ –CB[6] in phosphate buffer solution at 25 °C and mono-ammonium-CB[6] in 50% formic acid at 25 °C.<sup>[37]</sup>

$[\text{C}_n\text{mim}]\text{Br}$	$\Delta G$ [kJ mol <sup>-1</sup> ]	$\Delta H$ [kJ mol <sup>-1</sup> ]	$T \times \Delta S$ [kJ mol <sup>-1</sup> ]	$\log K_a$ [L mol <sup>-1</sup> ]	stoichiometry
$[\text{C}_2\text{mim}]\text{Br}$	–[a]	–[a]	–[a]	< 4	2:1 <sup>[23]</sup>
$[\text{C}_3\text{mim}]\text{Br}$	–[a]	–[a]	–[a]	< 4	–[a]
$[\text{C}_4\text{mim}]\text{Br}$	–29.3	–30.0	–0.7	5.1	1:1
$[\text{C}_5\text{mim}]\text{Br}$	–30.5	–31.1	–0.6	5.4	1:1
$[\text{C}_6\text{mim}]\text{Br}$	–25.9	–19.1	6.9	4.5	1:1
$[\text{C}_7\text{mim}]\text{Br}$	–[a]	–[a]	–[a]	< 4	–[a]
$[\text{C}_8\text{mim}]\text{Br}$	–[a]	–[a]	–[a]	< 4	–[a]
$[\text{C}_{12}\text{mim}]\text{Br}$	–[a]	–[a]	–[a]	< 4	–[a]
$\text{CH}_3\text{CH}_2\text{NH}_3^+$ <sup>[37]</sup>	–15.6	–4.6	11.0	2.73	1:1
$\text{CH}_3(\text{CH}_2)_2\text{NH}_3^+$ <sup>[37]</sup>	–21.2	–14.2	7.0	3.54	1:1
$\text{CH}_3(\text{CH}_2)_3\text{NH}_3^+$ <sup>[37]</sup>	–29.3	–26.8	–2.5	4.05	1:1
$\text{CH}_3(\text{CH}_2)_4\text{NH}_3^+$ <sup>[37]</sup>	–32.0	–27.4	–4.6	3.81	1:1
$\text{CH}_3(\text{CH}_2)_5\text{NH}_3^+$ <sup>[37]</sup>	–23.0	–22.1	0.9	3.83	1:1
$\text{CH}_3(\text{CH}_2)_6\text{NH}_3^+$ <sup>[37]</sup>	–15.2	–9.6	5.6	2.67	1:1

[a] Value could not be measured

host–guest binding strengths. For  $[\text{C}_2\text{mim}]\text{Br}$  and  $[\text{C}_3\text{mim}]\text{Br}$ , the binding constants are relatively weak and estimated to be lower than  $10^4 \text{ M}^{-1}$  which is consistent with fast exchange observed by  $^1\text{H NMR}$ . For  $[\text{C}_4\text{mim}]\text{Br}$  and  $[\text{C}_5\text{mim}]\text{Br}$ , the binding strengths are strong (above  $10^5 \text{ M}^{-1}$ ) and are in slow exchange in  $^1\text{H NMR}$  as discussed above. The binding constant for  $[\text{C}_6\text{mim}]\text{Br}$  is  $10^{4.5} \text{ M}^{-1}$  corresponding to an intermediate exchange on the NMR time scale. By extending the alkyl chain length to  $[\text{C}_7\text{mim}]\text{Br}$ , the binding strength is again too weak to be measured by ITC and appears to return to fast exchange in the  $^1\text{H NMR}$ . While high binding constants do not always indicate slow exchange in NMR, such as in the case of Istvan's work,<sup>[29]</sup> in our CB[6]-imidazolium system, the exchange rates are consistent with binding affinities.

From a thermodynamic point of view, the binding process is largely enthalpy driven. When the alkyl chains of  $[\text{C}_n\text{mim}]\text{Br}$  are longer than  $n=5$ , the value of association enthalpy decreases as illustrated in Table 2. A possible reason for this observed trend is that CB[6] has an interatomic distance of 6 Å between carbonyl oxygens axially spanning the cavity, which can optimally be filled by 4–5 methylene groups.<sup>[37]</sup> Consequently,  $[\text{C}_4\text{mim}]\text{Br}$  and  $[\text{C}_5\text{mim}]\text{Br}$  fit best inside the CB[6] cavity. For shorter chains, the hydrophobic effect is weaker, while for longer chains, the chain end, if fully extended, will exit the CB[6] cavity or require a backfolded conformation,<sup>[36]</sup> both of which are energetically unfavorable.

From the ITC experiments, the binding stoichiometry of  $[\text{C}_4\text{mim}]\text{Br}$ ,  $[\text{C}_5\text{mim}]\text{Br}$ , and  $[\text{C}_6\text{mim}]\text{Br}$  with CB[6] were all 1:1. In the absence of any buffers or salts,<sup>[34]</sup>  $[\text{C}_2\text{mim}]\text{Br}$  forms a 2:1 complex in solution with CB[6] as we reported previously.<sup>[23]</sup> Whether  $[\text{C}_3\text{mim}]\text{Br}$  will adopt a 2:1 binding stoichiometry with CB[6] is still unknown.

The binding constants and thermodynamic data of CB[6] and monoalkyl ammonium species with different chain lengths were measured by Buschmann (Table 2).<sup>[37]</sup> Although Buschmann's experiments were done in 50% formic acid, it has been suggested that the binding constants are nearly independent from the solvent acidity. The same trends were observed for both binding constants and enthalpy changes in our study with alkyl imidazoliums. While the highest binding constant for CB[6] with the monoalkyl ammonium series was found to be  $10^4 \text{ M}^{-1}$  for  $\text{CH}_3(\text{CH}_2)_3\text{NH}_3^+$ , the highest binding constant in our study is considerably higher,  $10^{5.35} \text{ M}^{-1}$  for  $[\text{C}_5\text{mim}]\text{Br}$ . This suggests that for the same alkyl chain length, the imidazolium series have a higher binding affinity for CB[6].

## Developing a Binding Model

Systematic movement of the chemical shifts in the  $^1\text{H NMR}$ , especially for protons  $\text{H}_c$  and  $\text{H}_d$ , verified two binding models (Figure 10). For  $[\text{C}_2\text{mim}]\text{Br}$ , the positive charge is partially located on the N3 atom, as shown in Figure 10a. The strong upfield shift of proton  $\text{H}_b$  indicates that a large part of the guest molecule ( $\text{H}_d$ ,  $\text{H}_e$ , and  $\text{H}_f$ ) has been embedded inside CB[6]'s shielding region.

Both nearest neighbor protons to N1,  $\text{H}_c$  on the alkyl chain and  $\text{H}_d$  on the imidazolium ring, were (on average) shifted upfield; this was caused by both the cavity shielding effect of CB[6] and the positive charge shielding effect from the localized charge existing on N3. Conversely,  $\text{H}_a$  on the

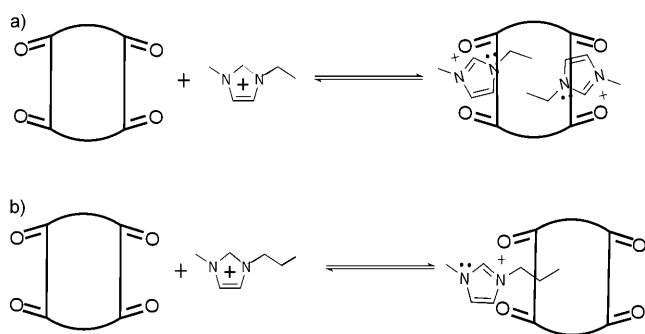


Figure 10. Two binding models of CB[6] with imidazolium.

N3 methyl group and  $H_c$  of the imidazolium ring, should experience a downfield shift caused by the positive charge inductive effect, however, these are not observed in the  $^1H$  NMR spectrum. In fact,  $H_c$  shifts slightly upfield and  $H_a$  remains almost unchanged. The lack of large chemical shifts in these cases can be rationalized by the downfield shifts being balanced out by shielding effects owing to the penetration depth for the smaller [C<sub>2</sub>mim]Br within the cavity of CB[6]. When considering a larger dialkylimidazolium guest, [C<sub>3</sub>mim]Br, the positive charge localizes closer to N1 in order to optimize both the hydrophobic effect and ion-dipole interactions as indicated in Figure 10b. Proton  $H_b$  exhibits a downfield shift suggesting that at least half of the imidazolium ring (N3 and C4 with  $H_c$ ) remains outside the portal region of CB[6] and thus is in the deshielding region. Compared with [C<sub>2</sub>mim]Br, the larger [C<sub>3</sub>mim]Br does not penetrate the CB[6] host as deeply. In this host-guest system, the positive charge should cause  $H_d$  and  $H_e$  to shift downfield while inducing an upfield shift in  $H_a$  and  $H_c$ . As the alkyl chain remains inside the CB[6] cavity, a strong shielding effect is dominant and  $H_e$  (and all other alkyl protons) experience an upfield shift. However, as  $H_d$  is located around the portal region, the shielding effect is not as strong as inside the cavity and the overall chemical shift is dominated by charge localization and the peak moves downfield. For  $H_a$  and  $H_c$ , the deshielding effect of CB[6] seems to dominate again over the positive charge effect as they both shift downfield. For [C<sub>4</sub>mim]Br through [C<sub>8</sub>mim]Br, the upfield and downfield shifts from  $H_a$  to  $H_f$  are identical to those observed for [C<sub>3</sub>mim]Br as described above.

When the length of the alkyl chain becomes much longer, as in [C<sub>12</sub>mim]Br, the proton  $H_f$  of the dodecyl chain end appeared to no longer reside inside the cavity of CB[6] evidenced by a slight downfield shift. On the other hand, proton  $H_b$  on the imidazolium ring moves upfield indicating the five-membered ring resides deeply inside the shielding area of CB[6], similar to [C<sub>2</sub>mim]Br.

## Conclusions

Binding properties between [C<sub>*n*</sub>mim]Br guest molecules with the macrocyclic host CB[6] were investigated with both

$1D$  and  $2D$  NMR techniques as well as ITC. A clear trend in binding with the length of the alkyl group on the N1 imidazolium position was observed. Upon binding, the N1 alkyl chain enters the hydrophobic cavity of CB[6] to maximize van der Waals interactions and the hydrophobic effect, while the positive charge on the imidazolium ring remains at the CB[6] portal region to maximize the ion-dipole interactions. For [C<sub>2</sub>mim]Br, the positive charge of the imidazolium ring is partially located on N3 to maximize both of these effects, however, as the ethyl chain is relatively short, a binding constant  $<10^4 M^{-1}$  and fast exchange on the NMR time scale were observed. From [C<sub>3</sub>mim]Br to [C<sub>8</sub>mim]Br, the positive charge on the ring becomes partially located on N1 as indicated by 2D NMR experiments. It was found that the tightest fit existed for butyl and pentyl alkyl chains; consequently, [C<sub>4</sub>mim]Br and [C<sub>5</sub>mim]Br have the strongest binding affinities with CB[6] ( $K_a > 10^5 M^{-1}$ ) and exhibit slow exchange on the NMR time scale. While longer alkyl chains still bind inside the CB[6] cavity, the energetics for this complexation are somewhat unfavorable and result in decreased binding affinities and intermediate and/or fast exchange on the NMR time scale. Finally, for substantially longer N3 alkyl chains, as in [C<sub>12</sub>mim]Br, the NMR behavior of its imidazolium ring resembles that of [C<sub>2</sub>mim]Br and a conformational rearrangement of the alkyl chain is likely to occur. This systematic investigation of alkyl chain penetration depth, charge localization, and a binding model for imidazolium-based guests inside CB[6] should serve as a useful guide for both synthetic and supramolecular chemists in designing and preparing novel functional self-organizing systems with CB[6] in neutral water.

## Experimental Section

### General

All chemicals used were of reagent grade or higher and used without further purification unless otherwise stated. 1-bromopentane (98%) and 1-bromohexane (98%) were obtained from Acros Organics. Ammonium hexafluorophosphate and tetraoctylammonium bromide were purchased from Alfa Aesar. 1-Butyl-3-methylimidazolium (97%) was supplied by Fluka. Tetrahydrofuran, dichloromethane, and diethyl ether were obtained from Fisher Scientific. 1-Methylimidazole (99%) was purchased from Lancaster. 1-Bromopropane (98%) was supplied by Avocado Organics. 1-Bromoheptane and 1-bromo-dodecane (96%) were purchased from Aldrich Chemicals. CB[6] was prepared using a one-pot reaction method.<sup>[8]</sup>

### Synthesis

**General Procedure for [C<sub>*n*</sub>mim]Br Synthesis:** For [C<sub>2</sub>mim]Br: 1-Methylimidazole (1.6 g, 20 mmol) and 1-bromoethane (4.5 g, 25 mmol) were refluxed in THF (tetrahydrofuran) for 72 h. The solvent was decanted and the residue was washed with diethyl ether and dried under vacuum yielding the title compound as a white crystalline solid (3.1 g, 80%).  $^1H$  NMR (400 MHz, D<sub>2</sub>O):  $\delta_H = 1.49$  (3H, t,  $J = 6$  Hz), 3.88 (3H, s), 4.22 (2H, q,  $J = 6$  Hz), 7.42 (1H, t,  $J = 1.6$  Hz), 7.49 (1H, t,  $J = 1.6$  Hz), 8.71 ppm (1H, s). Remaining characterization data is consistent with results previously published.<sup>[39]</sup>

[C<sub>3</sub>mim]Br was obtained as a transparent liquid (3.5 g, 86%).  $^1H$  NMR (400 MHz, D<sub>2</sub>O):  $\delta_H = 0.86$  (3H, t,  $J = 6$  Hz), 1.83 (2H, q,  $J = 6$  Hz), 3.84 (3H, s), 4.11 (2H, t,  $J = 5.6$  Hz), 7.38 (1H, t,  $J = 0.6$  Hz), 7.42 (1H, t,  $J =$

0.6 Hz), 8.66 ppm (1H, s). Remaining characterization data is consistent with results previously published.<sup>[39]</sup>

**[C<sub>5</sub>mim]Br** was obtained as a yellowish liquid (3.8 g, 80.7%). <sup>1</sup>H NMR (400 MHz, D<sub>2</sub>O):  $\delta_H$ =0.80 (3H, t,  $J$ =6 Hz), 1.22 (4H, m), 1.80 (2H, m,  $J$ =5.6 Hz), 3.82 (3H, s), 4.12 (2H, t,  $J$ =6 Hz), 7.36 (1H, t,  $J$ =1.6 Hz), 7.41 (1H, t,  $J$ =1.6 Hz), 8.64 ppm (1H, s). Remaining characterization data is consistent with results previously published.<sup>[39]</sup>

**[C<sub>6</sub>mim]Br** was obtained as a transparent liquid (4.0 g, 80.1%). <sup>1</sup>H NMR (400 MHz, D<sub>2</sub>O):  $\delta_H$ =0.81 (3H, t,  $J$ =4.4 Hz), 1.26 (6H, m), 1.85 (2H, m), 3.88 (3H, s), 4.18 (2H, t,  $J$ =5.6 Hz), 7.42 (1H, t,  $J$ =1.2 Hz), 7.47 (1H, t,  $J$ =1.6 Hz), 8.71 ppm (1H, s). Remaining characterization data is consistent with results previously published.<sup>[40]</sup>

**[C<sub>7</sub>mim]Br** was obtained as a transparent liquid (4.2 g, 79.6%). <sup>1</sup>H NMR (400 MHz, D<sub>2</sub>O):  $\delta_H$ =0.809 (3H, t,  $J$ =5.2 Hz), 1.23 (8 H, m), 1.83 (2H, m,  $J$ =5.6 Hz), 3.86 (3H, s), 4.15 (2H, t,  $J$ =5.6 Hz), 7.40 (1H, d,  $J$ =1.6 Hz), 7.44 (1H, d,  $J$ =1.6 Hz), 8.71 ppm (1H, s). Remaining characterization data is consistent with results previously published.<sup>[40]</sup>

**[C<sub>8</sub>mim]Br** was obtained as a transparent liquid (4.2 g, 79.6%). <sup>1</sup>H NMR (400 MHz, D<sub>2</sub>O):  $\delta_H$ =0.80 (3H, t,  $J$ =5.6 Hz), 1.23 (10 H, m), 1.82 (2H, m,  $J$ =5.6 Hz), 3.85 (3H, s), 4.15 (2H, t,  $J$ =5.7 Hz), 7.40 (1H, t), 7.43 (1H, t), 8.68 ppm (1H, s). Remaining characterization data is consistent with results previously published.<sup>[40]</sup>

**[C<sub>12</sub>mim]Br** was obtained as a white solid (5.4 g, 80.7%). <sup>1</sup>H NMR (400 MHz, D<sub>2</sub>O):  $\delta_H$ =0.78 (3H, t,  $J$ =5.7 Hz), 1.19 (14H, s), 1.27 (4H, s), 1.83 (2H, m), 3.88 (3H, s), 4.20 (2H, t,  $J$ =6.2 Hz), 7.48 (1H, d), 7.49 (1H, d), 8.88 ppm (1H, s). Remaining characterization data is consistent with results previously published.<sup>[40]</sup>

#### NMR Titration Experiments

<sup>1</sup>H NMR spectra were recorded on a Bruker DRX-400. HMBC spectra were recorded on a Bruker DRX-400 and NOESY spectra were recorded on a Bruker Avance 500. Chemical shifts are quoted in parts per million in aqueous solution. Samples with different ratios of CB[6] and [C<sub>n</sub>mim]Br ([H]/[G]) were prepared for titration experiments to reveal the binding properties between CB[6] and [C<sub>n</sub>mim]Br. CB[6] concentration was kept constant while the concentration of guest was varied with [H]/[G] ratios of 0.2, 0.4, 0.6, 0.8, and 1.0. The samples were prepared as follows: 10 mg mL<sup>-1</sup> [C<sub>n</sub>mim]Br solutions were prepared by dissolving [C<sub>n</sub>mim]Br in deuterium oxide. CB[6] (5 mg, 5 mmol) was weighed into a small sample vial. The calculated amount of imidazolium solution was injected into the same vial. Then deuterium oxide was added to the mixture to keep a total volume of 0.6 mL in all cases. After stirring for one hour, the sample solutions were transferred into NMR tubes. For 2D experiments, higher concentrations of CB[6] (25 mg, 25 mmol) and corresponding concentrations of the imidazolium guest were used.

#### ITC Titration Experiments

Titration experiments were carried out on a VP-ITC from Microcal Inc. at 25 °C in 10 mM sodium phosphate buffer (pH 7). The pH was checked periodically. Fresh analyte solutions were prepared every few days and were dissolved by sonication and heating up to 60 °C. All solutions were degassed prior to titration. The binding equilibria of all guests was studied using a cellular CB[6] concentration of 0.05 mM, to which a 0.6 mM guest solution was titrated. The guest in the injection syringe was added at a concentration of 1.0–2.0 mM. Typically 20–30 consecutive injections of 10–15  $\mu$ L were added, whereby the first injection was chosen to be 2  $\mu$ L in all cases. Thus the first data point was removed from the data set prior to curve fitting. Heats of dilution were found to be negligible in all cases. For binding constants larger than 10<sup>5</sup> M<sup>-1</sup>, heats of dilution were determined by titrating beyond saturation and subtracted from the data set. The data was analyzed with Origin 7.0 software, using the *one set of sites* model. A mean value from at least 3 measurements was used to determine the binding constants and heats of formation, unless otherwise stated. Reproducibility was tested using different batches of stock solutions of host, guest, and buffer. Deviations were found to be smaller than 6% for all binding constants.

## Acknowledgements

N.Z. gratefully acknowledges the Raymond and Helen Kwok Research Scholarship for financial support. F.B. thanks the German Academic Exchange Service (DAAD) for financial support. We thank all members in the Scherman Group for their helpful discussions.

- [1] R. Behrend, E. Meyer, F. Rusche, *Liebigs Ann. Chem.* **1905**, 339, 1–37.
- [2] W. A. Freeman, W. L. Mock, N. Shih, *J. Am. Chem. Soc.* **1981**, 103, 7367–7368.
- [3] N. J. Wheate, *Aust. J. Chem.* **2006**, 59, 354–354.
- [4] Y. H. Ko, E. Kim, I. Hwang, K. Kim, *Chem. Commun.* **2007**, 1305–1315.
- [5] J. Lagona, P. Mukhopadhyay, S. Chakrabarti, L. Isaacs, *Angew. Chem.* **2005**, 117, 4922–4949; *Angew. Chem. Int. Ed.* **2005**, 44, 4844–4870.
- [6] K. Kim, N. Selvapalam, D. H. Oh, *J. Inclusion Phenom. Macrocyclic Chem.* **2004**, 50, 31–36.
- [7] L. Isaacs, *Chem. Commun.* **2009**, 619–629.
- [8] J. Kim, I. Jung, S. Kim, E. Lee, J. Kang, S. Sakamoto, K. Yamaguchi, K. Kim, *J. Am. Chem. Soc.* **2000**, 122, 540–541.
- [9] S. Y. Jon, N. Selvapalam, D. H. Oh, J. Kang, S. Kim, Y. J. Jeon, J. W. Lee, K. Kim, *J. Am. Chem. Soc.* **2003**, 125, 10186–10187.
- [10] H. Buschmann, E. Cleve, K. Jansen, A. Wego, E. Schollmeyer, *Mater. Sci. Eng. C* **2001**, 14, 35–39.
- [11] H. Buschmann, K. Jansen, E. Schollmeyer, *Thermochim. Acta* **2000**, 346, 33–36.
- [12] W. L. Mock, N. Shih, *J. Org. Chem.* **1983**, 48, 3618–3619.
- [13] W. L. Mock, N. Shih, *J. Org. Chem.* **1986**, 51, 4440–4446.
- [14] Y. Jeon, J. Kim, D. Whang, K. Kim, *J. Am. Chem. Soc.* **1996**, 118, 9790–9791.
- [15] R. Hoffmann, W. Knoche, C. Fenn, H. Buschmann, *J. Chem. Soc. Faraday Trans.* **1994**, 90, 1507–1511.
- [16] H. J. Buschmann, E. Cleve, E. Schollmeyer, *Inorg. Chim. Acta* **1992**, 193, 93–97.
- [17] G. Zhang, Z. Xu, S. Xue, Q. Zhu, Z. Tao, *Wuji Huaxue Xuebao* **2003**, 19, 655–659.
- [18] H. Buschmann, E. Cleve, K. Jansen, E. Schollmeyer, *Anal. Chim. Acta* **2001**, 437, 157–163.
- [19] H.-J. Buschmann, E. Cleve, K. Jansen, A. Wego, E. Schollmeyer, *J. Inclusion Phenom. Macrocyclic Chem.* **2001**, 40, 117–120.
- [20] X. X. Zhang, K. E. Krakowiak, G. Xue, J. S. Bradshaw, R. M. Izatt, *Ind. Eng. Chem. Res.* **2000**, 39, 3516–3520.
- [21] H. Buschmann, K. Jansen, C. Meschke, E. Schollmeyer, *J. Solution Chem.* **1998**, 27, 135–140.
- [22] R. M. Izatt, R. E. Terry, B. L. Haymore, L. D. Hansen, N. K. Dalley, A. G. Avondet, J. J. Christensen, *J. Am. Chem. Soc.* **1976**, 98, 7620–7626.
- [23] L. Liu, N. Zhao, O. A. Scherman, *Chem. Commun.* **2008**, 1070–1072.
- [24] T. Welton, *Chem. Rev.* **1999**, 99, 2071–2083.
- [25] A. Paul, P. K. Mandal, A. Samanta, *J. Phys. Chem. B* **2005**, 109, 9148–9153.
- [26] R. F. de Souza, J. C. Padilha, R. S. Goncalves, J. Rault-Berthelot, *Electrochem. Commun.* **2006**, 8, 211–216.
- [27] P. Nockemans, K. Binnemans, K. Driesen, *Chem. Phys. Lett.* **2005**, 415, 131–136.
- [28] P. A. Hunt, B. Kirchner, T. Welton, *Chem. Eur. J.* **2006**, 12, 6762–6775.
- [29] M. Zsombor, B. Laszlo, M. Monika, J. Istvan, *J. Phys. Chem. B* **2009**, 113, 1645–1651.
- [30] R. Wang, L. Yuan, D. Macartney, *Chem. Commun.* **2006**, 2908–2910.
- [31] N. Noujeim, L. Leclercq, A. R. Schmitzer, *J. Org. Chem.* **2008**, 73, 3784–3790.
- [32] L. Leclercq, N. Noujeim, S. H. Sanon, A. R. Schmitzer, *J. Phys. Chem. B* **2008**, 112, 14176–14184.

- [33] S. Samsam, L. Leclercq, A. R. Schmitzer, *J. Phys. Chem. B* **2009**, *113*, 9493–9498.
- [34] V. Kolman, R. Marek, Z. Strelcova, P. Kulhanek, M. Necas, J. Svec, V. Sindelar, *Chem. Eur. J.* **2009**, *15*, 6926–6931.
- [35] L. Liu, N. Nouvel, O. A. Scherman, *Chem. Commun.* **2009**, 3243–3245.
- [36] Y. H. Ko, H. Kim, Y. Kim, K. Kim, *Angew. Chem.* **2008**, *120*, 4174–4177; *Angew. Chem. Int. Ed.* **2008**, *47*, 4106–4109.
- [37] C. Meschke, H. J. Buschmann, E. Schollmeyer, *Thermochim. Acta* **1997**, *297*, 43–48.
- [38] C. A. Schalley, *Analytical Methods in Supramolecular Chemistry*, Wiley-VCH, **2007**.
- [39] E. R. Parnham, R. E. Morris, *Chem. Mater.* **2006**, *18*, 4882–4887.
- [40] J. M. Obliosca, S. D. Arco, M. H. Huang, *J. Fluoresc.* **2007**, *17*, 613–618.

Received: September 29, 2009  
Published online: February 8, 2010